Numerical Solution of Heat Transfer Flow in Micropolar Nanofluids with Oxide Nanoparticles in Water and Kerosene Oil about a Horizontal Circular Cylinder

Hamzeh T. Alkasasbeh, Mohammed Z. Swalmeh, Abid Hussanan, Mustafa Mamat

Abstract— In this paper, the heat transfer flow of a micropolar nanofluid mixture containing three types of oxide nanoparticles namely titanium oxide (TiO_2), alumina oxide (Al_2O_3) and graphene oxide (GO) which suspended in two different types of fluids such as water and kerosene oil are investigated over a heated horizontal circular cylinder with constant surface heat flux. The dimensionless form of governing equations are solved via an implicit finite difference scheme known as Keller-box method. The effects of nanoparticles volume fraction, Prandtl number, micro-rotation parameter on temperature, velocity and angular velocity are plotted and discussed. Further, numerical results for the local wall temperature and the local skin friction coefficient are obtained. It is found that the local wall temperature of Al_2O_3 based nanofluid is higher than the other oxide based nanofluid, but the local skin friction of GO is higher than the other oxide nanoparticles, for every values of nanoparticle volume fraction and micro-rotation parameter. The present results of local wall temperature and local skin friction for Newtonian fluid are found to be in good agreement with the literature.

Index Terms—Circular Cylinder; Heat Transfer; Micropolar Nanofluid; Oxide Nanoparticles.

I. INTRODUCTION

Micropolar fluids, a subclass of microfluids are considered to be a special kind of suspensions described by micropolar theories. Eringen [1] was the first who introduced the theory of micropolar fluids, in which the stress tensor is no longer symmetric but rather an anti-symmetric characteristic due to the oriented micro-rotation of particles. Later on, a substantial study has been done on the micropolar fluid to explore the important results related to different flow problems. Agarwal et al. [2] considered micropolar heat transfer flow past a stationary porous wall.

Manuscript received August 4, 2018; revised May, 5, 2019.

This work is supported by the Ton Duc Thang University, Ho Chi Minh City, Vietnam

H. T. Alkasasbeh, Department of Mathematics, Faculty of Science, Ajloun National University, P.O. Box 43, Ajloun 26810, Jordan. (e-mail: hamzahtahak@yahoo.com)

M. Z. Swalmeh, Faculty of Informatics and Computing, Universiti Sultan Zainal Abidin (Kampus Gong Badak), 21300 Kuala Terengganu, Terengganu, Malaysia; Faculty of Arts and Sciences, Aqaba University of Technology, Aqaba-Jordan.

A. Hussanan, Division of Computational Mathematics and Engineering, Institute for Computational Science, Ton Duc Thang University, Ho Chi Minh City, Vietnam; Faculty of Mathematics and Statistics, Ton Duc Thang University, Ho Chi Minh City, Vietnam.

Corresponding Author Email: abidhussanan@tdtu.edu.vn

M. Mamat, Faculty of Informatics and Computing, Universiti Sultan Zainal Abidin (Kampus Gong Badak), 21300 Kuala Terengganu, Terengganu, Malaysia.

Chemical reaction and heat absorption/generation effects on free convection flow over a stretched permeable surface was investigated by Rebhi et al. [3]. Bachok et al. [4] considered flow of a micropolar fluid over an unsteady stretching sheet. Unsteady MHD mixed convection periodic flow of a micropolar fluid with thermal radiation and chemical reaction was examined by Pal and Talukdar [5]. They used perturbation technique as the main tool to obtain analytically solutions. Turkyilmazoglu [6] considered micropolar fluid heat transfer flow due to a porous stretching sheet. Micropolar forced convection flow over moving surface under magnetic field was reported by Waqas et al. [7]. Micropolar fluid unsteady free convection flow over a vertical plate with Newtonian heating is considered by Hussanan et al. [8]. Hussanan et al. [9] obtained an exact solution of heat and mass transfer in micropolar fluid over an oscillating vertical plate under Newtonian heating effects. Alkasasbeh [10] presented the numerical solution on heat transfer magnetohydrodynamic flow of micropolar casson fluid over a horizontal circular cylinder with thermal radiation using Keller-box method

In past decades, different techniques have been used to improve the rate of heat transfer to reach different level of thermal efficiencies. To achieve this object, the enhancement of thermal conductivity is very important. Choi [11] was the first who conducted the research on enhancement of heat transfer in convectional fluids through suspended nanoparticles (with sizes significantly smaller than 100 nm). Nanofluids are a new type of working fluids containing uniformly dispersed and suspended metallic or nonmetallic nanoparticles. After the revolutionary work, this research topic has attracted the attention of many researchers due to its fascinating thermal characteristics and potential applications. Two mathematical models have been used to study the characteristics of nanofluids, namely, Buongiorno model [12] and Tiwari-Das model [13]. Buongiorno approach focuses on Brownian diffusion and thermophoresis mechanisms. Daniel et al. [14] determined slip thermal radiation effects on unsteady MHD natural convection flow of nanofluid over a shrinking sheet. In view of its great importance, many authors have used this model in the analysis of nanofluid flow, for example, Noreen et al. [15]; Boulahia et al. [16]; Qasim et al. [17]; Wakif et al. [18]; Afridi and Qasim [19].

On the other hand, Tiwari-Das model considered nanoparticles volume fraction instead of the Brownian motion and thermophoresis effects. In recent years, there are some interesting results obtained by many researchers by using this model. The flow of water based nanofluids past a wedge with partial slip was analysed by Rahman et al. [20].

Sheremet et al. [21] considered thermal stratification on free convection in a square porous cavity filled with nanofluid. Unsteady MHD flow of some nanofluids through porous medium over an accelerated vertical plate was investigated by Hussanan et al. [22]. Chen et al. [23] disclosed the analysis of the nanofluid flow in a porous channel with suction and chemical reaction. Sheikholeslami [24] considered magnetic field on water based nanofluid with Fe3O4 nanoparticles. Sheikholeslami [25] continued with the same model and investigated the influence of coulomb forces on Fe3O4 suspended water based nanofluid in a cavity with moving wall. Hussanan et al. [26] investigated the natural convection flow of micropolar nanofluid over a vertical plate. They analyzed the impact of oxide nanoparticles on water, kerosene and engine oil based nanofluids. Flow of Casson sort of nanofluid over a vertical plate with leading edge accretion/ablation using sodium alginate as a base fluid has been considered by Hussanan [27]. Hussanan et al. [28] also studied microstructure and inertial characteristics of a magnetite ferrofluid using micropolar fluid model. Swalmeh et al. [29] highlighted the impacts of natural convection on boundary layer flow of Cu-water and Al_2O_3-water micropolar nanofluid about a solid sphere. Influence of the mixed convection oxide nanoparticles based micropolar nanofluid by Alkasasbeh et al. [30]

To the best of author's knowledge, the problem of flow of water and kerosene oil based micropolar nanofluid suspended by titanium oxide (TiO_2), alumina oxide (Al_2O_3) and graphene oxide (GO) over a heated horizontal circular cylinder has not been investigated by any researcher up till now. To fill out the gap, heat transfer flow of a micropolar nanofluid mixture containing copper and silver nanoparticles are considered over a heated horizontal circular cylinder. A similarity transformation is used to convert the governing equations into a nonlinear ordinary differential equations, which are solved via an implicit finite difference scheme known as Keller-box method.

II. MATHEMATICAL ANALYSES

Consider the free convection over a heated horizontal circular cylinder of radius *a*, which is immersed in a steady laminar two-dimensional incompressible and viscous micropolar nanofluid of TiO_2, Al_2O_3 and GO in two different types of base fluids such as water and Kerosene oil are considered in a constant surface heat flux.

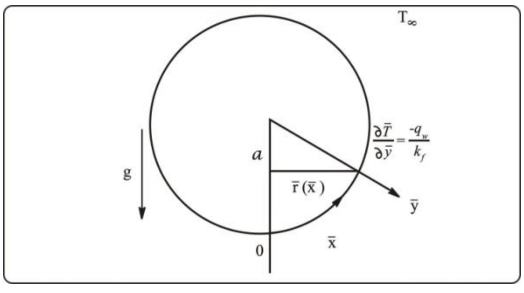

Fig. 1. Physical model and coordinate system

In figure 1 the surface temperature of the cylinder is $T_w > T_\infty$ the ambient temperature of the fluid which remains unchanged, and the gravity vector g acts downward in the opposite direction, where $\bar{x}-$coordinate is measured along the circumference of the horizontal circular cylinder from the lower stagnation point, $\bar{y}-$coordinate is measured normal to the surface of the circular cylinder. The incompressible fluid model which is approximated by the Boussinesq model, the governing equations for the laminar natural convection in terms of the continuity, momentum, energy and micro-rotation equations for a micropolar nanofluid, respectively.

$$\frac{\partial \bar{u}}{\partial \bar{x}} + \frac{\partial \bar{v}}{\partial \bar{y}} = 0, \tag{1}$$

$$\rho_{nf}\left(\bar{u}\frac{\partial \bar{u}}{\partial \bar{x}} + \bar{v}\frac{\partial \bar{u}}{\partial \bar{y}}\right) = \left(\mu_{nf}+\kappa\right)\frac{\partial^2 \bar{u}}{\partial \bar{y}^2} + \rho_{nf}\left(\chi\rho_s\beta_s + (1-\chi)\rho_f\beta_f\right)g\left(T-T_\infty\right)\sin\left(\frac{\bar{x}}{a}\right) + \kappa\frac{\partial \bar{H}}{\partial \bar{y}}, \tag{2}$$

$$\bar{u}\frac{\partial T}{\partial \bar{x}} + \bar{v}\frac{\partial T}{\partial \bar{y}} = \alpha_{nf}\frac{\partial^2 T}{\partial \bar{y}^2}, \tag{3}$$

$$\rho_{nf}\, j\left(\bar{u}\frac{\partial \bar{H}}{\partial \bar{x}} + \bar{v}\frac{\partial \bar{H}}{\partial \bar{y}}\right) = -\kappa\left(2\bar{H} + \frac{\partial \bar{u}}{\partial \bar{y}}\right) + \phi_{nf}\frac{\partial^2 \bar{H}}{\partial \bar{y}^2}, \tag{4}$$

subject the boundary conditions defined by Nazar et al. [31] as

$$\bar{u} = \bar{v} = 0,\ \frac{\partial T}{\partial \bar{y}} = \frac{-q_w}{k}, \bar{H} = -\frac{1}{2}\frac{\partial \bar{u}}{\partial \bar{y}} \text{ as } \bar{y} = 0, \quad \bar{u}\to 0,\ T\to T_\infty,\ \bar{H}\to 0, \text{ as } \bar{y}\to\infty, \tag{5}$$

where $\bar{u}$ and $\bar{v}$ are the velocity components along with the $\bar{x}$ and $\bar{y}$ axes, $j = a^2 Gr^{-2/5}$ is micro-inertia density, All other symbols and quantities are displayed in nomenclature. The ρ_{nf} is the density of the nanofluid, μ_{nf} is the viscosity of the nanofluid and α_{nf} is the thermal diffusivity of the nanofluid. Which are defined by Tham et al. [32] as

$$\rho_{nf} = (1-\chi)\rho_f + \chi\rho_f,\ \mu_{nf} = \frac{\mu_f}{(1-\chi)^{2.5}}, \quad \left(\rho c_p\right)_{nf} = (1-\chi)\left(\rho c_p\right)_f + \chi\left(\rho c_p\right)_s, \quad \frac{k_{nf}}{k_f} = \frac{\left(k_s+2k_f\right)-2\chi\left(k_f-k_s\right)}{\left(k_s+2k_f\right)+\chi\left(k_f-k_s\right)},\ \alpha_{nf} = \frac{k_{nf}}{\left(\rho c_p\right)_{nf}}, \tag{6}$$

where χ is the nanoparticles volume fraction, $\chi = 0$ correspond to a regular fluid. In order to simplify the mathematical analysis of the problem, we introduce the following non-dimensional variables (Nazar et al. [30])

$$x = \frac{\bar{x}}{a},\ y = Gr^{1/5}\left(\frac{\bar{y}}{a}\right), r = \frac{\bar{r}}{a},\ u = \left(\frac{a}{\nu_f}\right)Gr^{-2/5}\bar{u}, \quad v = \left(\frac{a}{\nu_f}\right)Gr^{-1/5}\bar{v}, H = \left(\frac{a^2}{\nu_f}\right)Gr^{-3/5}\bar{H}, \quad \theta = Gr^{1/5}\left(\frac{T-T_\infty}{aq_w/k}\right), \tag{7}$$

where $Gr = g\beta_f\left(aq_w/k\right)\left(a^3/\nu_f^2\right)$ is the Grashof number for prescribed wall temperature conditions, and the spin gradient viscosity of nanofluid $\phi_{nf} = \left(\mu_{nf}+\kappa/2\right)j$. Substituting equations (6) and (7) into equations (1) to (4) obtains to the following non-dimensional equations

$$\frac{\partial u}{\partial x}+\frac{\partial v}{\partial y}=0, \tag{8}$$

$$u\frac{\partial u}{\partial x}+v\frac{\partial u}{\partial y}=\frac{\rho_f}{\rho_{nf}}\left(D(\chi)+K\right)\frac{\partial^2 u}{\partial y^2}+ \frac{1}{\rho_{nf}}\left(\chi\rho_s\left(\frac{\beta_s}{\beta_f}\right)+(1-\chi)\rho_f\right)\theta\sin x+\frac{\rho_f}{\rho_{nf}}K\frac{\partial H}{\partial y}, \tag{9}$$

$$u\frac{\partial \theta}{\partial x}+v\frac{\partial \theta}{\partial y}=\frac{1}{\Pr}\left[\frac{k_{nf}/k_f}{(1-\chi)+\chi(\rho c_p)_s/(\rho c_p)_f}\right]\frac{\partial^2\theta}{\partial y^2}, \tag{10}$$

$$u\frac{\partial H}{\partial x}+v\frac{\partial H}{\partial y}=-\frac{\rho_f}{\rho_{nf}}K\left(2H+\frac{\partial u}{\partial y}\right)+ \frac{\rho_f}{\rho_{nf}}\left(D(\chi)+\frac{K}{2}\right)\frac{\partial^2 H}{\partial y^2}, \tag{11}$$

where, $D(\chi)=(1-\chi)^{-2.5}$, $\Pr=\nu_f/\alpha_f$ is the Prandtl number, and $K=\kappa/\mu_f$ is micro-rotation parameter, The boundary condition (5) becomes

$$u=v=0,\ \theta=-1,\ H=-\frac{1}{2}\frac{\partial u}{\partial y}\ \text{at}\ y=0,$$
$$u\to 0,\ \theta\to 0,\ H\to 0,\ \text{as}\ y\to\infty. \tag{12}$$

we assume the following variables

$$\psi=xf(x,y),\ \theta=\theta(x,y),\ H=xh(x,y), \tag{13}$$

where ψ is the stream function defined as

$$u=\frac{\partial \psi}{\partial y}\ \text{and}\ v=-\frac{\partial \psi}{\partial x}, \tag{14}$$

which satisfies the continuity equation (8). Substituting equations (13), (14) into (9) to (11) becomes to the following equations

$$\frac{\rho_f}{\rho_{nf}}\left(D(\chi)+K\right)\frac{\partial^3 f}{\partial y^3}+f\frac{\partial^2 f}{\partial y^2}-\left(\frac{\partial f}{\partial y}\right)^2 +\frac{1}{\rho_{nf}}\left(\chi\rho_s\left(\frac{\beta_s}{\beta_f}\right)+(1-\chi)\rho_f\right)\frac{\sin x}{x}\theta +\frac{\rho_f}{\rho_{nf}}K\frac{\partial h}{\partial y}=x\left(\frac{\partial f}{\partial y}\frac{\partial^2 f}{\partial x\partial y}-\frac{\partial f}{\partial x}\frac{\partial^2 f}{\partial y^2}\right), \tag{15}$$

$$\frac{1}{\Pr}\left[\frac{k_{nf}/k_f}{(1-\chi)+\chi(\rho c_p)_s/(\rho c_p)_f}\right]\frac{\partial^2\theta}{\partial y^2}+f\frac{\partial \theta}{\partial y}= x\left(\frac{\partial f}{\partial y}\frac{\partial \theta}{\partial x}-\frac{\partial f}{\partial x}\frac{\partial \theta}{\partial y}\right), \tag{16}$$

$$\frac{\rho_f}{\rho_{nf}}\left(D(\chi)+\frac{K}{2}\right)\frac{\partial^2 h}{\partial y^2}+f\frac{\partial h}{\partial y}-\frac{\partial f}{\partial y}h -\frac{\rho_f}{\rho_{nf}}K\left(2h+\frac{\partial^2 f}{\partial y^2}\right)=x\left(\frac{\partial f}{\partial y}\frac{\partial h}{\partial x}-\frac{\partial f}{\partial x}\frac{\partial h}{\partial y}\right), \tag{17}$$

subject to the boundary conditions

$$f=\frac{\partial f}{\partial y}=0,\ \theta=-1,\ h=-\frac{1}{2}\frac{\partial^2 f}{\partial y^2}\ \text{at}\ y=0,$$
$$\frac{\partial f}{\partial y}\to 0,\ \theta\to 0,\ h\to 0\ \text{as}\ y\to\infty. \tag{18}$$

It can be observed that at the lower stagnation point of the circular cylinder, $(x\approx 0)$, equations result to the following ordinary differential equations

$$\frac{\rho_f}{\rho_{nf}}\left(D(\chi)+K\right)f'''+ff''-\left(\frac{\partial f}{\partial y}\right)^2 +\frac{1}{\rho_{nf}}\left(\chi\rho_s\left(\frac{\beta_s}{\beta_f}\right)+(1-\chi)\rho_f\right)\theta+\frac{\rho_f}{\rho_{nf}}K\frac{\partial h}{\partial y}=0, \tag{19}$$

$$\frac{1}{\Pr}\left[\frac{k_{nf}/k_f}{(1-\chi)+\chi(\rho c_p)_s/(\rho c_p)_f}\right]\theta''+f\theta'=0, \tag{20}$$

$$\frac{\rho_f}{\rho_{nf}}\left(D(\chi)+\frac{K}{2}\right)h''+fh'-\frac{\partial f}{\partial y}h-\frac{\rho_f}{\rho_{nf}}K\left(2h+f''\right)=0. \tag{21}$$

The boundary conditions become

$$f(0)=f'(0)=0,\ \theta'(0)=-1,$$
$$h(0)=-\frac{1}{2}f''(0)\ \text{as}\ y=0, \tag{22}$$
$$f'\to 0,\ \theta\to 0,\ h\to 0\ \text{as}\ y\to\infty,$$

where primes denote differentiation with respect to y, $\Pr$ is the Prandtl number [34, 35, 36]. In particle applications, the local skin friction coefficient C_f and the wall temperature θ_w, which are written by

$$C_f=\left(D(\chi)+\frac{K}{2}\right)x\frac{\partial^2 f}{\partial y^2}(x,0),\ \theta_w=\theta(x,0). \tag{23}$$

III. NUMERICAL SOLUTION

Equations (15) to (17) subject to boundary conditions (18) are solved numerically using the Keller-box method. This method seems to be the most flexible of the common methods and despite recent developments in other numerical methods, remains a powerful and very accurate approach for parabolic boundary layer flows. It is also being easily adaptable to solve equations of any order and unconditionally stable on the solutions. The solution is obtained by the following four steps

i. Reduce the transformed equations (15) to (17) to a first-order system.
ii. Write the difference equations using central differences.
iii. Linearize the resulting algebraic equations by Newton's method and write them in matrix- vector form.
iv. Solve the linear system by the block tridiagonal elimination technique.

In this paper, numerical solutions start at the lower stagnation point of the cylinder, $(x\approx 0)$, and proceed around the cylinder up to the separation point. The step size Δy in y, and the edge of the boundary layer y_∞ had to be adjusted for different values of parameters to maintain accuracy. Therefore, we have used the step size of $\Delta y=0.02$ and $\Delta x=0.005$ in the present study.

IV. RESULTS AND DISCUSSION

The steady free convection flow of micropolar nanofluid is investigated over a circular cylinder. Three types of oxide nanoparticles namely titanium oxide (TiO_2), alumina oxide (Al_2O_3) and graphene oxide (GO) are suspended in two different types of base fluids such as water and kerosene oil. Thermo-physical properties of based fluids and oxide nanoparticles are given in Table 1.

TABLE 1
THERMOPHYSICAL PROPERTIES OF BASED FLUIDS AND NANOPARTICLES [26, 32]

Physical properties	Water	Kerosene oil	TiO_2	Al_2O_3	GO
ρ (kg/m^3)	997.1	783	4250	3970	1800
C_p (J/kg–K)	4179	2090	686.2	765	717
K (W/m–K)	0.613	0.145	8.9538	40	5000
$\beta\times10^{-5}(K^{-1})$	21	99	0.9	0.85	28.4
Pr	6.2	21	…..	…..	…..

TABLE 2
COMPARISON OF LOCAL WALL TEMPERATURE θ_w FOR VISCOUS NEWTONIAN FLUID WITH $\Pr=1$, $K=0$ AND $\chi=0$

x	Merkin and Pop [33]	Nazar et al. [31]	Present
0	1.996	1.996	1.9964
0.2	1.999	1.999	1.9985
0.4	2.005	2.004	2.0039
0.6	2.014	2.013	2.0127
0.8	2.026	2.026	2.0258
1.0	2.043	2.044	2.0436
1.2	2.064	2.065	2.0654
1.4	2.089	2.091	2.0908
1.6	2.120	2.123	2.1225
1.8	2.158	2.161	2.1609
2.0	2.202	2.207	2.2064
2.2	2.256	2.262	2.2612
2.4	2.322	2.329	2.3289
2.6	2.403	2.413	2.4128
2.8	2.510	2.523	2.5219
3.0	2.660	2.681	2.6807
π	2.824	2.828	2.8284

TABLE 3
COMPARISON OF LOCAL SKIN FRICTION COEFFICIENT C_f FOR VISCOUS NEWTONIAN FLUID WITH $\Pr=1$, $K=0$ AND $\chi=0$

x	Merkin and Pop [33]	Nazar et al. [31]	Present
0	0.0000	0.0000	0.0000
0.2	0.274	0.273	0.2732
0.4	0.541	0.540	0.5399
0.6	0.793	0.795	0.7947
0.8	1.031	1.027	1.0280
1.0	1.241	1.235	1.2351
1.2	1.422	1.413	1.4190
1.4	1.567	1.555	1.5667
1.6	1.671	1.657	1.6679
1.8	1.732	1.714	1.7296
2.0	1.744	1.723	1.7394
2.2	1.704	1.680	1.6988
2.4	1.608	1.580	1.5959
2.6	1.451	1.418	1.4447
2.8	1.225	1.188	1.2181
3.0	0.913	0.868	0.9046
π	0.613	0.574	0.6068

The governing equations have been solved via Keller box method and the results are shown in several plots for the effects of different parameters such as the micro-rotation parameter K and nanoparticles volume fraction on local wall temperature, local skin friction coefficient, temperature, velocity and angular velocity fields. The numerical results of nonlinear partial differential equations start at the lower stagnation point of the circular cylinder $x\approx0$, with initial profiles as given by the equations (19) to (21), and proceed round of the circumference of circular cylinder up to $x=\pi$. The comparison of present results with previously published results reported by Merkin and Pop [33] and Nazar et al. [31] are made in Tables 2 and 3. We found that present results are in a good agreement.

The impact of nanoparticles volume fraction χ and the micro-rotation parameter K on the local Wall temperature Nu and local skin friction C_f with several values of x for TiO_2, Al_2O_3 and Go nanoparticles based in water and kerosene oil are shown in Figures 2 to 5. It is found that the local wall temperature θ_w and the local skin friction coefficient C_f increase with increasing values of nanoparticles volume fraction χ and micro-rotation parameter K. It is also found that the local wall temperature θ_w for Al_2O_3 is higher than the other oxide nanoparticles for every value of nanoparticles volume fraction χ and micro-rotation parameter K. Further, the local skin friction C_f of Go is higher than other oxide nanoparticles for each values nanoparticles volume fraction χ and micro-rotation parameter K. It is also noticed that there is a sharp rise in the local wall temperature θ_w for Al_2O_3-water as compare to TiO_2-kerosene oil.

The results of temperature, velocity and angular velocity profiles for TiO_2 and GO dispersed in kerosene oil with various values of χ and K are given in Figures 6 to 11, respectively. The results show that an increase in nanoparticles volume fraction χ and micro-rotation parameter K leads to an increase in temperature and velocity field and a decrease in the angular velocity. It is also found that the temperature and velocity of TiO_2-kerosene oil is higher than GO-kerosene oil, but the angular velocity of GO-kerosene oil is higher than that of TiO_2-kerosene oil for every values nanoparticles volume fraction χ and micro-rotation parameter K. It is also noticed from Figure 7 that there is a sharp fall in the velocity field within the layer $y<2$ and then it becomes uniform for both nanoparticles as $y\to\infty$.

Figures 12 to 17, illustrate the effect of nanoparticles volume fraction χ and micro-rotation parameter K on temperature, velocity, and angular velocity for GO nanoparticles in two different base fluids such as water and kerosene oil. It is found that when χ and K increases, the temperature and velocity profiles increase, but the angular velocity profiles decreases. It is true because volume of GO increases when thermal conductivity increases and then thickness of thermal boundary layer also increases. In addition, it is also found that for each value of nanoparticles volume fraction χ, the thermal boundary thickness of GO - water based nanofluid is greater than GO-kerosene based nanofluid. On the other hand, GO-water has high temperature and velocity compared with GO-kerosene and GO-water has low angular velocity as compare to GO-kerosene oil. It is examined from Figure 15 that GO nanoparticles suspended kerosene oil based micropolar nanofluid exhibits relatively less temperature than that of GO water based nanofluid within the layer $y<3$ and then it becomes uniform for both water and kerosene oil as $y \to \infty$.

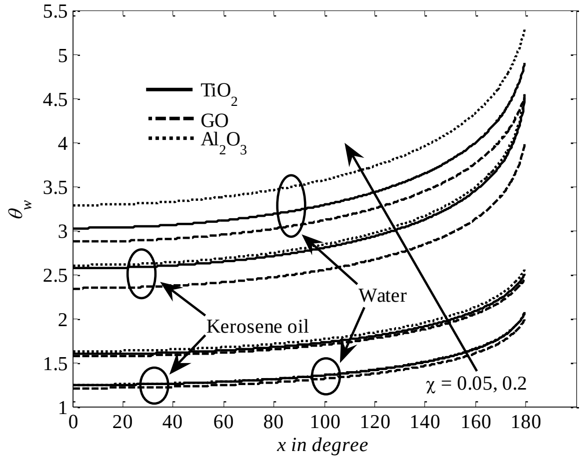

Fig. 2. Variation of local wall temperature for different based fluids with TiO_2, Al_2O_3 and GO nanoparticles for various values of x and χ when $K = 0.2$

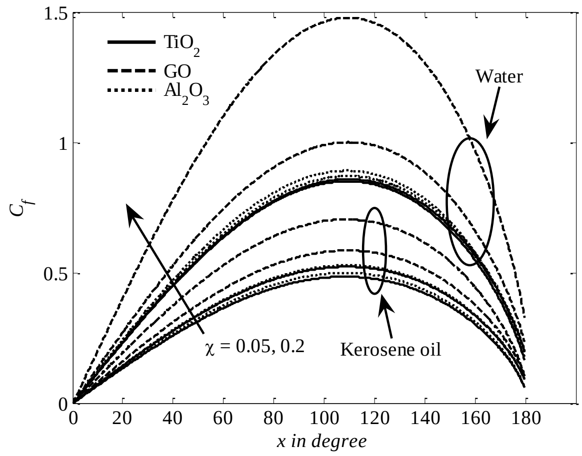

Fig. 3. Variation of local skin friction for different based fluids with TiO_2, Al_2O_3 and GO nanoparticles for various values of x and χ when $K = 0.2$

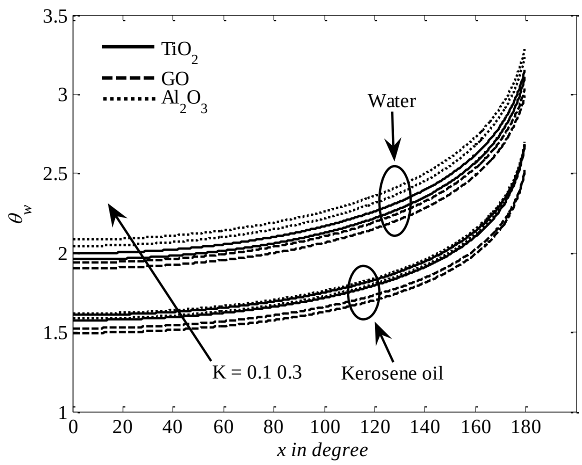

Fig. 4. Variation of local wall temperature for different based fluids with TiO_2, Al_2O_3 and GO nanoparticles for various values of x and K when $\chi = 0.1$

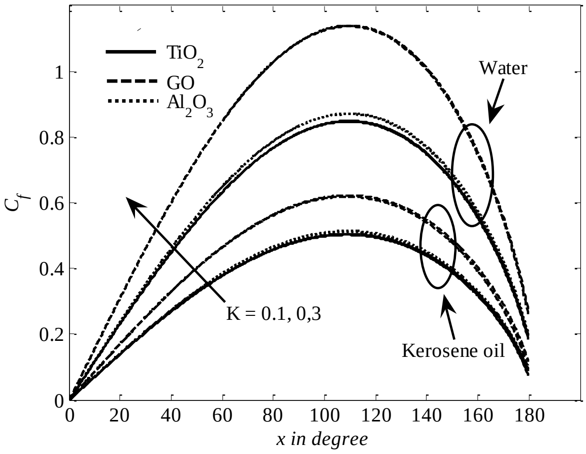

Fig. 5. Variation of local skin friction for different based fluids with TiO_2, Al_2O_3 and GO nanoparticles for various values of x and K when $\chi = 0.1$

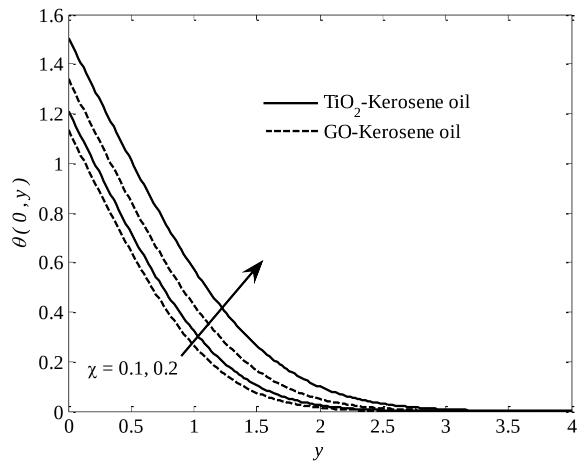

Fig. 6. Variation of temperature for kerosene oil based nanofluids with TiO_2 and GO nanoparticles for various values of x and χ when $K = 0.1$

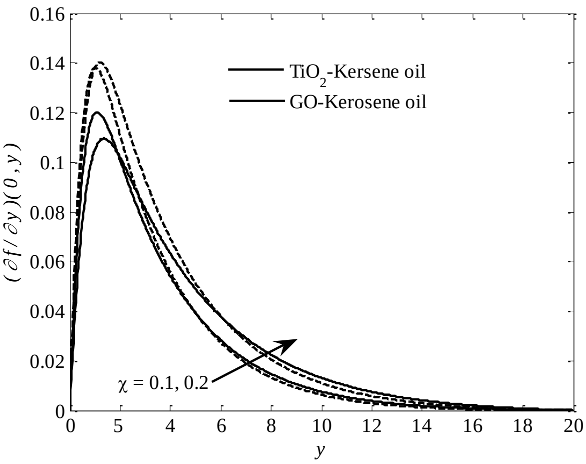

Fig. 7. Variation of velocity for kerosene oil based nanofluids with TiO_2 and GO nanoparticles for various values of x and χ when $K = 0.1$

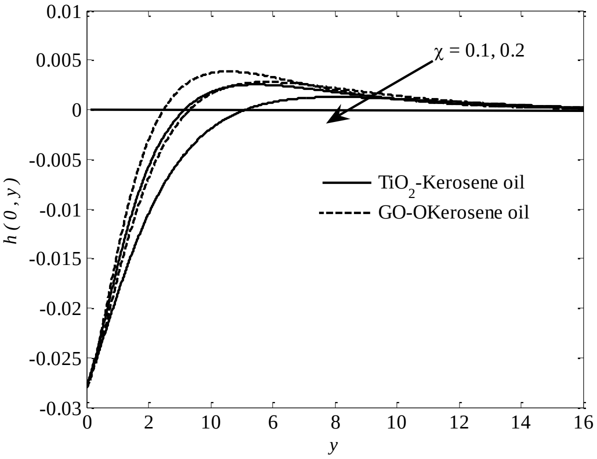

Fig. 8. Variation of angular velocity profile for kerosene oil based nanofluids with TiO_2 and GO nanoparticles for various values of *x* and χ when $K = 0.1$

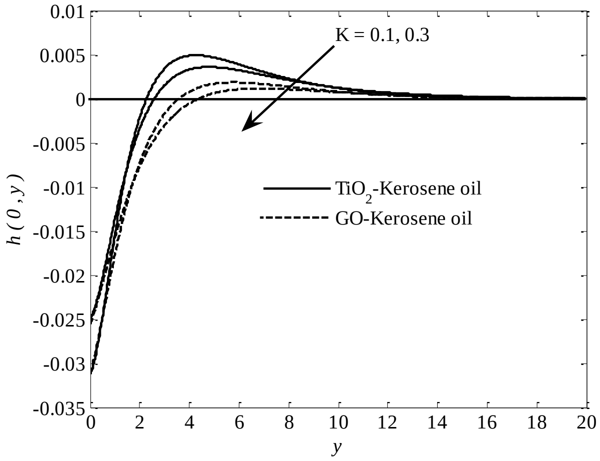

Fig. 11. Variation of angular velocity field for kerosene oil based nanofluids with TiO_2 and GO nanoparticles for various values of *x* and K when $\chi = 0.1$

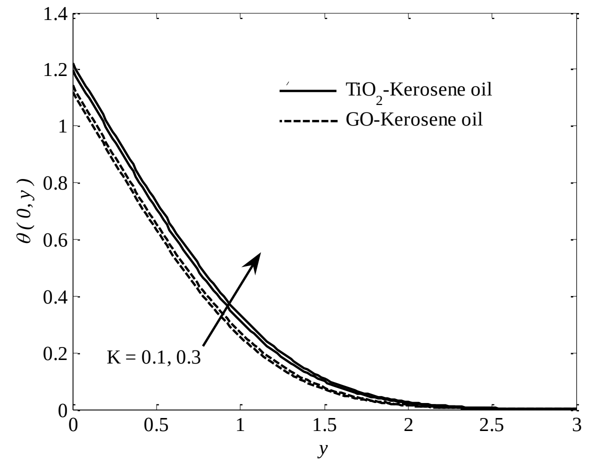

Fig. 9. Variation of temperature for kerosene oil based nanofluids with TiO_2 and GO nanoparticles for various values of *x* and K when $\chi = 0.1$.

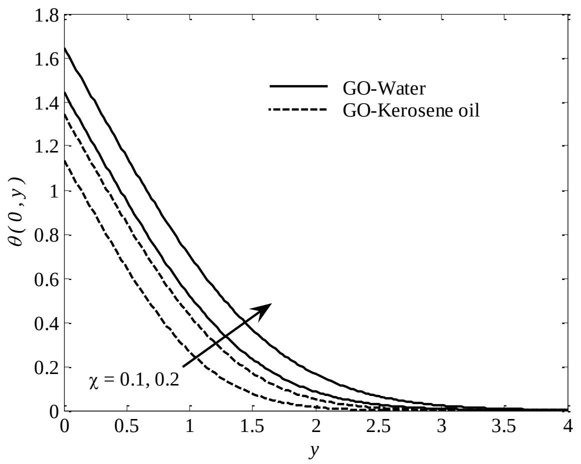

Fig. 12. Variation of temperature for different based fluids with GO nanoparticle for various values of *y* and χ, when $K = 0.2$

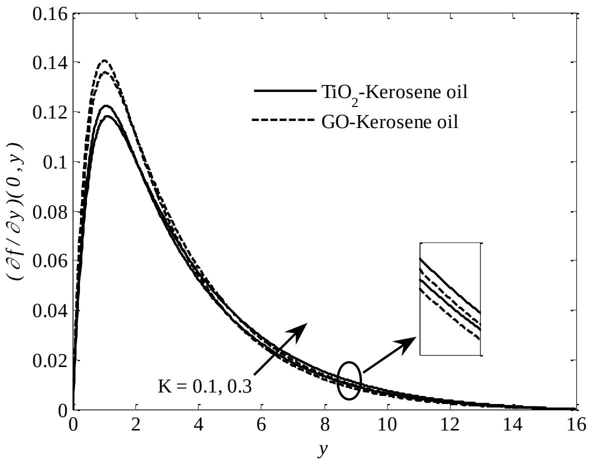

Fig. 10. Variation of velocity for kerosene oil based nanofluids with TiO_2 and GO nanoparticles for various values of *x* and K when $\chi = 0.1$.

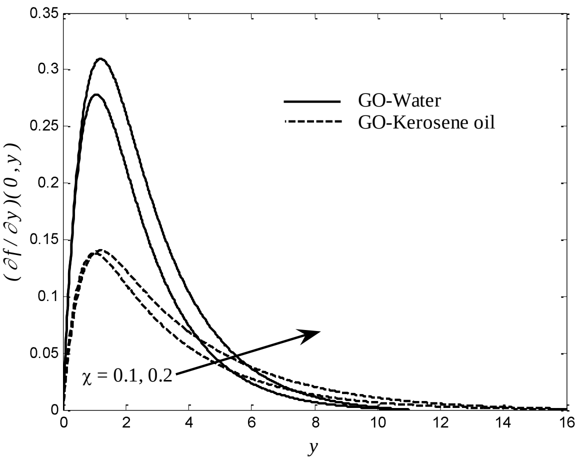

Fig. 13. Variation of velocity for different based fluids with GO nanoparticle for various values of *y* and χ, when $K = 0.2$

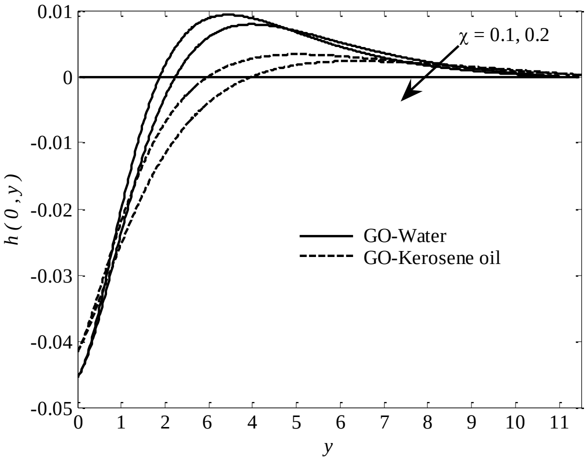

Fig. 14. Variation of the angular velocity field for different based fluids with GO nanoparticle for various values of *y* and χ, when $K = 0.2$

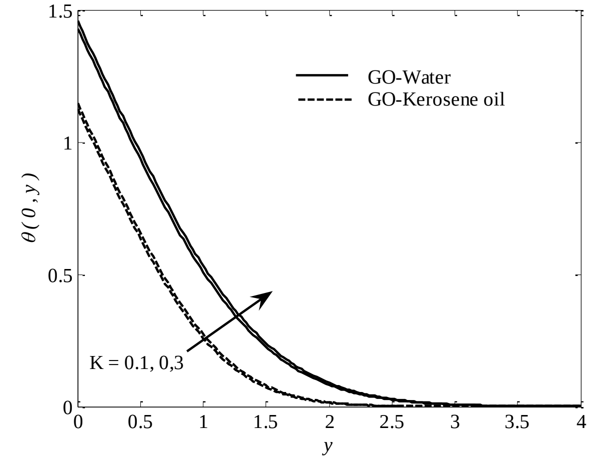

Fig. 15. Variation of temperature for different based fluids with GO nanoparticle for various values of *y* and K, when $\chi = 0.1$

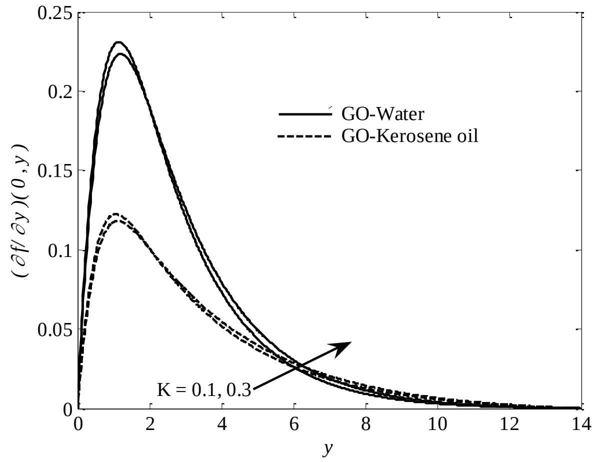

Fig. 16. Variation of the velocity field for different based fluids with GO nanoparticle for various values of *y* and K when $\chi = 0.1$

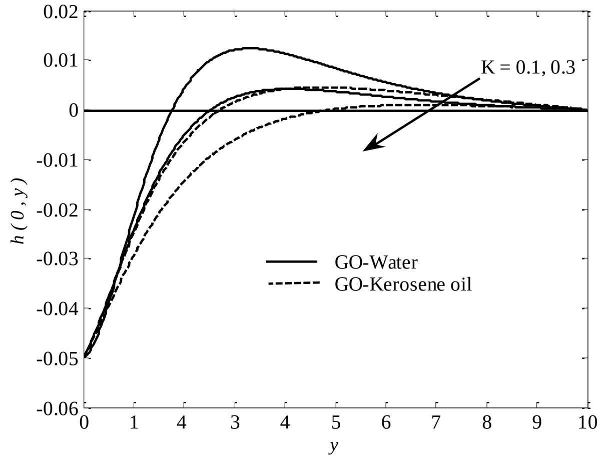

Fig. 17. Variation of the angular velocity field for different based fluids with GO nanoparticle for various values of *y* and K when $\chi = 0.1$

V. CONCLUSIONS

The present study investigates the natural convection heat transfer of oxide nanoparticles namely TiO_2, Al_2O_3 and GO suspended micropolar nanofluid within horizontal circular cylinder immersed with constant heat flux. The main concluding remarks are presented below:

i. The local wall temperature of Al_2O_3 based nanofluid is higher than the other oxide based nanofluid, but the local skin friction of GO is higher than the other oxide nanoparticles, for every values nanoparticle volume fraction and the micro-rotation parameter.
ii. TiO_2-kerosene oil is higher than GO-kerosene oil in temperature and velocity profiles, but in the angular velocity profiles, the GO-kerosene oil is higher than TiO_2-kerosene oil, for every values nanoparticle volume fraction and micro-rotation parameter.
iii. The value of temperature and velocity profiles GO-water has high temperature and velocity profiles compared with GO-Kerosene, and GO-water has low angular velocity profile with GO-Kerosene oil.
iv. When the nanoparticles volume fraction χ and micro-rotation K parameter increases the temperature and velocity increases and decrease in angular velocity profiles.

ACKNOWLEDGEMENTS

The corresponding author would like to thanks Ton Duc Thang University, Ho Chi Minh City, Vietnam for the financial support.

REFERENCES

[1] A. C. Eringen, "Theory of micropolar fluids," *Journal of Applied Mathematics and Mechanics*, vol. 16, no.2 pp. 1-18, 1966.

[2] R. S. Agarwal, R. Bhargava, and A.V.S. Balaji, "Numerical solution of flow and heat transfer of a micropolar fluid at a stagnation point on a porous stationary wall," *Indian Journal of Pure and Applied Mathematics*, vol. 21, pp. 567-573, 1990.

[3] A. D. Rebhi, M. Q. Al-Odat, J. C. Ali, and A. S. Benbella, "Combined effect of heat generation or absorption and first-order chemical reaction on micropolar fluid flows over a uniformly stretched permeable surface," *International Journal of Thermal Sciences*, vol. 48, no. 8, pp. 1658-1663, 2009.

[4] N. Bachok, A. Ishak, and R. Nazar, "Flow and heat transfer over an unsteady stretching sheet in a micropolar fluid," *Meccanica*, vol. 46, no. 5, pp. 935-942, 2011.
[5] D. Pal, and B. Talukdar, "Perturbation technique for unsteady MHD mixed convection periodic flow, heat and mass transfer in micropolar fluid with chemical reaction in the presence of thermal radiation," *Central European Journal of Physics*, vol. 10, no. 5, pp. 1150-1167, 2012.
[6] M. Turkyilmazoglu, "Flow of a micropolar fluid due to a porous stretching sheet and heat transfer. International Journal of Non-Linear," *Mechanics*, vol. 83, pp. 59-64, 2016.
[7] H. Waqas, S. Hussain, H. Sharif, and S. Khalid, "MHD forced convective flow of micropolar fluids past a moving boundary surface with prescribed heat flux and radiation," *British Journal of Mathematics & Computer Science*, vol. 21, pp. 1-14, 2017.
[8] A. Hussanan, M. Z. Salleh, I. Khan, and R. M. Tahar, "Unsteady Free Convection Flow of a Micropolar Fluid with Newtonian Heating: Closed form Solution," *Thermal Science*, vol. 21, pp. 2307-2320, 2017.
[9] A. Hussanan, M. Z. Salleh, I. Khan, and R. M. Tahar, "Heat and mass transfer in a micropolar fluid with Newtonian heating: An exact analysis," *Neural Computing and Applications*, vol. 29, no. 6, pp. 59-67, 2018.
[10] H. T. Alkasasbeh, "Numerical solution on heat transfer magnetohydrodynamic flow of micropolar casson fluid over a horizontal circular cylinder with thermal radiation," *Frontiers in Heat and Mass Transfer (FHMT)*, vol. 10. pp. 1-7, 2018.
[11] S. U. S. Choi, "Enhancing thermal conductivity of fluids with nanoparticles," *ASME International Mechanical Engineering Congress and Exposition*, vol. 231, no. pp. 99-105, 1995.
[12] J. Buongiorno, "Convective transport in nanofluids," *ASME Journal of Heat Transfer*, vol. 128, no 12, pp. 240-250, 2006.
[13] R. K. Tiwari, and M. K. Das, "Heat transfer augmentation in a two-sided lid-driven differentially heated square cavity utilizing nanofluids," *International Journal of Heat and Mass Transfer*, vol. 50, no. 9-10, pp. 2002-2018, 2007.
[14] Y. S. Daniel, Z. A. Aziz, Z. Ismail, and F. Salah, "Slip effects on electrical unsteady MHD natural convection flow of nanofluid over a permeable shrinking sheet with thermal radiation," *Engineering Letters*, vol. 26, no. 1, pp. 107-116, 2018.
[15] S. Noreen, M. M. Rashidi, and M. Qasim, "Blood flow analysis with considering nanofluid effects in vertical channel," *Applied Nanoscience*, vol. 7, no. 5, pp. 193-199, 2017.
[16] Z. Boulahia, A. Wakif, and R. Sehaqui, "Finite volume analysis of free convection heat transfer in a square enclosure filled by a Cu-water nanofluid containing different shapes of heating cylinder," *Journal of Nanofluids*, vol. 6, no. 4, pp. 1-8, 2017.
[17] M. Qasim, Z. H. Khan, I.Khan, and Q. M. Al-Mdallal, "Analysis of entropy generation in flow of methanol-based nanofluid in a sinusoidal wavy channel," *Entropy*, vol. 19, no. 10, pp. 490-501, 2017.
[18] A. Wakif, Z. Boulahia, and R. Sehaqui, "A semi-analytical analysis of electro-thermo-hydrodynamic stability in dielectric nanofluids using Buongiorno's mathematical model together with more realistic boundary conditions," *Results in Physics*. vol. 9, pp.1438-1454, 2018.
[19] M. I. Afridi, and M. Qasim, "Comparative study and entropy generation analysis of Cu-H2O and Ag-H2O nanofluids flow over a slendering stretching surface," *Journal of Nanofluids,* 7, no. 4, pp. 783-790, 2018.
[20] M. M. Rahman, M. A. Al-Lawatia, I. A. Eltayeb, and N. Al-Salti, "Hydromagnetic slip flow of water based nanofluids past a wedge with convective surface in the presence of heat generation (or) absorption," *International Journal of Thermal Sciences*, vol. 57, pp. 172-182, 2012.
[21] M. A. Sheremet, S. Dinarvand, and I. Pop, "Effect of thermal stratification on free convection in a square porous cavity filled with a nanofluid using Tiwari and Das' nanofluid model," *Physica E*, vol. 69, pp. 332-341, 2015.
[22] A. Hussanan, I. Khan, H. Hashim, M. K. A. Mohamed, N. Ishak, N. M. Sarif, and M. Z. Salleh, "Unsteady MHD flow of some nanofluids past an accelerated vertical plate embedded in a porous medium," *Jurnal Teknologi*, vol. 78, no. 2, pp. 121-126, 2016.
[23] H. Chen, T. Xiao, and M. Shen, "Nanofluid flow in a porous channel with suction and chemical reaction using Tiwari and Das's nanofluid model," *Heat Transfer-Asian Research*, vol. 46, no. 7, pp. 1-12, 2016.
[24] M. Sheikholeslami, "Magnetic source impact on nanofluid heat transfer using CVFEM," *Computing and Applications*, vol. 30, no. 4, pp. 1055-1064. 2016.
[25] M. Sheikholeslami, "Influence of Coulomb forces on Fe_3O_4-H_2O nanofluid thermal improvement," *International Journal of Hydrogen Energy* vol. 42, no. 2, pp. 821-829. 2017.
[26] A. Hussanan, M. Z. Salleh, I. Khan, and S. Shafie, "Convection heat transfer in micropolar nanofluids with oxide nanoparticles in water, kerosene and engine oil," *Journal of Molecular Liquids,* vol. 229, no. pp. 482-488. 2017.
[27] A. Hussanan, S. Aman, Z. Ismail, M. Z. Salleh, and B.Widodo, "Unsteady natural convection of sodium alginate viscoplastic Casson based nanofluid flow over a vertical plate with leading edge accretion/ablation," *Journal of Advanced Research in Fluid Mechanics and Thermal Sciences*. vol. 45, no. 1, pp. 92-98, 2018.
[28] A. Hussanan, M. Z. Salleh, and I. Khan, "Microstructure and inertial characteristics of a magnetite ferrofluid over a stretching/shrinking sheet using effective thermal conductivity model," *Journal of Molecular Liquids,* vol. 255, pp. 64-75, 2018.
[29] M. Z. Swalmeh, H. T. Alkasasbeh, A. Hussanan, and Mamat, M. "Heat transfer flow of Cu-water and Al2O3-water micropolar nanofluids about a solid sphere in the presence of natural convection using Keller-box method," *Results in Physics* vol. 9, pp. 717-724, 2018.
[30] H. T. Alkasasbeh, M. Z. Swalmeh, A. Hussanan, Mamat M "Effects of Mixed Convection on Methanol and Kerosene Oil Based Micropolar Nanofluid Containing Oxide Nanoparticles, " *Akademia Baru/ CFD Letters;* vol 11 no. 1, pp 55-66, 2019.
[31] R. Nazar, N. Amin, T. Grosan, and I. Pop. "Free convection boundary layer on a horizontal circular cylinder with constant surface heat flux in a micropolar fluid," *International Journal Applied Mechanics & Engineering,* vol. 7, no. 2, pp. 409-431, 2002.
[32] L. Tham, R. Nazar, and I Pop, "Mixed convection boundary layer flow from a horizontal circular cylinder in a nanofluid," *International Journal of Numerical Methods for Heat & Fluid Flow;* vol. 22, no. 5, pp. 576–606, 2012.
[33] J. H. Merkin, and I. Pop, "A Note on the free convection boundary layer on a horizontal circular with constant heat flux," *Wärme- und Stoffübert*. vol. 22, no. 1-2, pp. 79 81, 1988.
[34] A. A. Opanuga, J. A. Gbadeyan, and S. A. Iyase, "Second law analysis of hydromagnetic couple stress fluid embedded in a non-Darcian porous medium," *IAENG International Journal of Applied Mathematics*, vol. 47, no.3, pp287-294, 2017.
[35] A. N. Kashif, Z. A. Aziz, F. Salah, and K. K. Viswanathan, "Convective heat transfer in the boundary layer flow of a Maxwell fluid over a flat plate using an approximation technique in the presence of pressure gradient," *Engineering Letters*, vol. 26, no. 1, pp. 14-22, 2018.
[36] A. Hussanan, I. Khan, M. R. Gorji, and W. A. Khan, "CNTs water-based nanofluid over a stretching sheet," *BioNanoScience,* https://doi.org/10.1007/s12668-018-0592-6, 2019.